A Simple Near-Capacity Concatenation Scheme Over MISO Channels

Nghi H. Tran, Tho Le-Ngoc, Tad Mastumoto, and Ha H. Nguyen

Abstract— **This paper proposes a capacity-approaching, yet simple scheme over a multiple-input single-output (MISO) wireless fading channel, which is very common in the downlink of a cellular system. The proposed scheme is based on a concatenation of a mixture of short memory-length convolutional codes or repetition codes and a short, and simple rate-1 linear block code, followed by either 1-dimensional (1-D) anti-Gray or Gray mapping of quadrature phase-shift keying (QPSK) modulation. By interpreting rate-1 code together with 1-D mapping as a multi-D mapping performed over multiple transmit antennas, the error performance is analyzed in the turbo pinch-off region using EXIT chart. At first, a simple design criterion on the bit-wise mutual information with perfect *a priori* information is derived. Based on the obtained design criterion, an optimal rate-1 code for each 1-D mapping is then constructed to maximize the bit-wise mutual information with perfect *a priori* information. The combination of optimal rate-1 code and 1-D mapping results in a steep inner detector's EXIT curve over an MISO channel, which matches very well to that of a simple outer code. It is demonstrated that the simple concatenation scheme can achieve a near-capacity performance over the MISO channels. In some cases, the selected mixed code is just a simple repetition code.**

Index Terms— **Multiple-input single-output (MISO) channels, capacity-approaching performance, EXIT chart, convolutional code, repetition code, block code.**

I. Introduction

It is widely known that the use of multiple antennas significantly enhances the error performance of a wireless system [1], [2]. With the recent developments in iterative decoding, a number of pragmatic approaches using powerful turbo-like codes have been proposed [3], [4] to achieve a close-capacity performance under a bit-interleaved coded modulation (BICM) framework [5], [6]. For instance, by using a turbo code as an outer code, it was shown in [3] that a near-capacity performance can be attained in a symmetric antenna setup where the number of receive antennas equals the number of transmit antennas. This result also holds in an antenna setup where the number of receive antennas is greater than the number of transmit antennas.

This work was supported in parts by the Natural Sciences and Engineering Research Council of Canada (NSERC), and by the Japanese government funding program, Grant-in-Aid for Scientific Research (B), No. 20360168.

Nghi H. Tran and Tho Le-Ngoc are with the Department of Electrical & Computer Engineering, McGill University, Montreal, Quebec, Canada. Email: nghi.tran@mcgill.ca, tho@ece.mcgill.ca.

Tad Mastumoto is with Japan Advanced Institute of Science and Technology, Japan, and Center for Wireless Communication at University of Oulu, Finland. Email: matumoto@jaist.ac.jp.

Ha H. Nguyen is with the Department of Electrical & Computer Engineering, University of Saskatchewan, Saskatchewan, Canada. Email: ha.nguyen@usask.ca.

In a practical wireless system, it might not be feasible to implement multiple antennas at both the transmitter and receiver. It is due to the reason that a multiple-antenna system requires multiple radio frequency chains and low-noise amplifiers, which is very costly. Furthermore, in some applications such as the downlink of a cellular system, it is physically not possible to place multiple antennas on a small handset. Under this antenna configuration, the design for a capacity-approaching system is much more challenging. For example, it was observed in [7], [8] that the error performance of a coded system using turbo codes or low-density parity check (LDPC) codes optimized for the binary-input channels experiences a severe degradation when the antenna setup is asymmetric, e.g., there is only a single antenna at the receiver. The problem can be overcome by using orthogonal space-time block codes in order to transfer a multiple antenna channel into single-input single-output channels [8]. Unfortunately, a complex orthogonal design with full transmission rate does not exist for more than two transmit antennas. Recently, by using a very well-design irregular LDPC code followed by Gray mapping with QPSK, reference [4] proposes a coded modulation scheme that performs very close to the capacity limit in the asymmetric antenna setup with four transmit antennas. Using a similar approach as in [4], equally good performances are also obtained in [9] by using outer irregular repeat accumulate (RA) codes. To our knowledge, the designs in [4], [9] are still the most effective coded modulation techniques for near-capacity performance over wireless fading channels under the asymmetric antenna configuration.

As an alternative, this paper proposes a simple yet effective concatenation scheme with QPSK over an asymmetric multiple-antenna channels in which multiple antennas are only equipped at the transmitter. This antenna configuration is very common in the downlink of a cellular system. The proposed system is based on a simple serial concatenation of a mixture of short memory-length convolutional codes or repetition codes and a short rate-1 linear block code and applicable for both 1-D anti-Gray or Gray mapping. By interpreting rate-1 code together with 1-D mapping as a multi-D mapping employed over multiple transmit antennas, the error performance is analyzed in the turbo pinch-off region for a close-capacity performance using extrinsic information transfer (EXIT) chart [4], [10], [11]. In particular, a simple design criterion on the bitwise mutual information with perfect *a priori* information is first developed. This derivation allows us to determine optimal rate-1 linear block codes for anti-Gray and Gray mappings to maximize the bitwise mutual information with perfect *a priori* information. The most suitable outer mixed codes are

Digital Object Identifier: 10.4108/ICST.BROADNETS2009.7271
http://dx.doi.org/10.4108/ICST.BROADNETS2009.7271

then selected to match to the inner detector with a steep-slope EXIT curve. Analytical and simulation results indicate that the simple concatenation scheme approaches near-capacity. In some cases, the selected mixed code is just a simple repetition code.

It should be noted that this paper assumes the ergodic fading channel and only the receiver but not the transmitter knows the channel. Furthermore, as similar to [3], [4], a direct transmission over multiple transmit antennas is considered without the use of special multiple-antenna code-design such as space-time codes [12]–[15]. It is certainly interesting to further extend the technique proposed in this paper to cover both spatial and temporal domains.

II. System Model

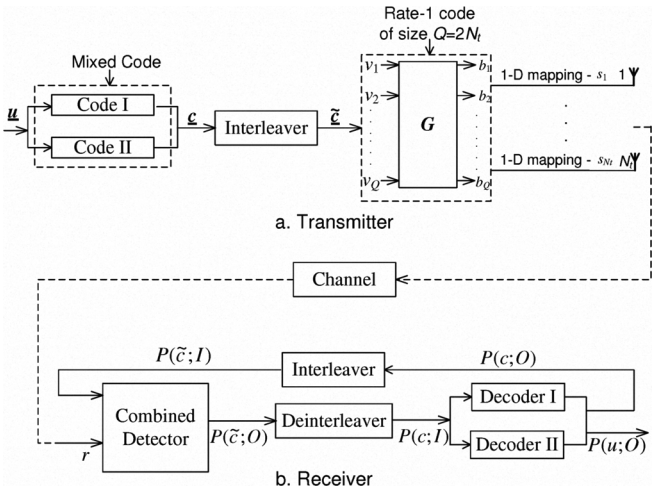

Fig. 1. The proposed concatenation scheme equipped with N_t transmit antennas and one receive antenna.

A. Transmitter

A block diagram of the transmitter of the proposed concatenation system equipped with $N_t > 1$ transmit antennas and $N_r = 1$ receive antenna is depicted in Fig. 1 (a)[1]. First, a binary information block $\boldsymbol{u}$ of length L_u is divided into two binary sequences $\boldsymbol{u}_I$ and $\boldsymbol{u}_{II}$ of lengths L_I and L_{II}, respectively. Each sequence $\boldsymbol{u}_l$, $l \in \{I, II\}$, is encoded by a suitable rate-k_l/n_l binary encoder into a coded sequence $\boldsymbol{c}_l$ consisting of $T_l = L_l n_l / k_l$ coded bits. These binary encoders could be simple convolutional or repetition codes and shall be determined later. A coded sequence $\boldsymbol{c}$ of length $T_c = T_I + T_{II}$ is then constructed by serially combining coded sequences $\boldsymbol{c}_I$ and $\boldsymbol{c}_{II}$. This encoding structure, inherited from the code doping technique proposed in [18], [19], is referred to as a mixed code of $K = 2$ binary codes, with code doping ratio $\alpha = L_I/L_u$. As shall be shown later, this mixed code provides a flexible structure to control the convergence behavior of the system. Note that the number of binary encoders can be straightforwardly generalized to $K > 2$. Furthermore, the use of a single outer convolutional or repetition code is a special case of the proposed mixed code.

After being interleaved, each group of $Q = 2N_t$ coded bits of interleaved sequence $\tilde{c}$, denoted as $\boldsymbol{v} = (v_1, v_2, \ldots, v_Q)^\top$, is fed to a simple rate-1 linear block code with generator matrix $\boldsymbol{G}$ of size $Q \times Q$ over Galois filed 2 (GF(2)). The design of this rate-1 code is discussed in the next section. A vector of Q output coded bits $\boldsymbol{b} = (b_1, b_2, \ldots, b_Q)^\top$ is given as:

$$\boldsymbol{b} = \boldsymbol{G} \cdot \boldsymbol{v}. \tag{1}$$

In (1), all operations are defined over GF(2). The linearity of $\boldsymbol{G}$ is to guarantee that there is one-to-one correspondence between $\boldsymbol{v}$ and $\boldsymbol{b}$. Then two consecutive bits (b_{2i-1}, b_{2i}), $1 \le i \le N_t$, are grouped together and mapped to a complex QPSK symbol s_i using either 1-D anti-Gray or Gray mapping. A sequence of N_t 1-D complex symbols $\{s_i\}$ is considered to be a super symbol $\boldsymbol{s} = [s_1, s_2, \ldots, s_{N_t}]^\top$ in an N_t-D constellation $\boldsymbol{\Psi}$ with cardinality $|\boldsymbol{\Psi}| = 2^Q$. Each component s_i is finally transmitted by the ith transmit antenna.

The combination of rate-1 linear block code and 1-D mapping above can be interpreted as a special case of multi-D mapping technique in which a vector of Q binary bits $\boldsymbol{v} = [v_1, v_2, \ldots, v_Q]^\top$ are mapped directly to a super symbol $\boldsymbol{s}$ according to some multi-D mapping rule [20], [21]. Hereafter, vector $\boldsymbol{v}$ is referred to as the label of $\boldsymbol{s}$. The optimal choices of rate-1 code as well as an outer mixed code for a near-capacity performance shall be discussed shortly in the next section.

B. Receiver

Consider an ergodic frequency-flat Rayleigh fading channel. The received signal r is given as:

$$r = \boldsymbol{h}^\top \cdot \boldsymbol{s} + n. \tag{2}$$

In (2), the vector $\boldsymbol{h}$ is an $N_t \times 1$ complex vector known perfectly at the receiver and its components are $\mathcal{CN}(0,1)$[2]. Furthermore, n is $\mathcal{CN}(0, N_0)$ representing additive white Gaussian noise (AWGN).

At the receiver, a typical concatenation of a conventional detector, *a posteriori* probability (APP) bit decoder of rate-1 block code, and a soft-input soft-output (SISO) outer decoder can be applied. Similar to the design in [9], the detector and rate-1 block decoder can be combined in one block as shown in Fig. 1 (b) to reduce decoding complexity and improve robustness. More specifically, by representing rate-1 block code and 1-D mapping as a multi-D mapping ξ, the optimal combined detector performs APP detection to provide the extrinsic probability of the k coded bit v_k, $1 \le k \le Q$, being set at b, $b \in \{0, 1\}$, as:

$$P(v_k = b; O) = \sum_{\boldsymbol{s} \in \boldsymbol{\Psi}_b^k} \left[\exp\left(-\frac{||r - \boldsymbol{h} \cdot \boldsymbol{s}||^2}{N_0} \right) \cdot \prod_{j \neq k} P\left(v_j = v_j(\boldsymbol{s}); I\right) \right]. \tag{3}$$

[1] In [16], [17], we have generalized the scheme to an asymmetric antenna setup in which $N_t > N_r$.

[2] Here $\mathcal{CN}(0, \sigma^2)$ denotes a circularly symmetric complex Gaussian random variable with variance $\sigma^2/2$ per dimension.

Digital Object Identifier: 10.4108/ICST.BROADNETS2009.7271
http://dx.doi.org/10.4108/ICST.BROADNETS2009.7271

In (3), $\mathbf{\Psi}_b^k$ denotes a subset of $\mathbf{\Psi}$ that contains all symbols whose labels have the value b at the kth position. Clearly, $\mathbf{\Psi}_b^k$ is determined by the mapping rule ξ. Furthermore, $v_j(\boldsymbol{s})$ is the value of the jth bit in the label of $\boldsymbol{s}$ and $P\left(v_j = v_j(\boldsymbol{s}); I\right)$ is the *a priori* probability of the other bits, $j \neq k$, on the same channel symbol. Observe that the computation of the extrinsic information of the coded bit in (3) involves the set of 2^{Q-1} super symbols in $\mathbf{\Psi}_b^k$, which has the same complexity as that of the conventional detector [3], [4].

After being deinterleaved, the extrinsic information of the corresponding T_I and T_{II} coded bits computed by the combined detector is forwarded to the two SISO channel decoders, respectively. For convolutional codes, the SISO channel decoder uses the forward-backward algorithm [22], [23]. If the binary encoder is a rate-$1/n$ repetition code, the extrinsic information for each coded bit is simply calculated as:

$$P(c_i = b; O) = \prod_{j=1, j\neq i}^{n} P\left(c_j = b; I\right). \tag{4}$$

There is an iterative processing between the combined detector and the outer channel decoder to exchange the extrinsic information of the coded bits $P(v; O)$ and $P(c; O)$. After being interleaved, $P(v; O)$ and $P(c; O)$ become the *a priori* information $P(c; I)$ and $P(v; I)$ at the input of the SISO decoder and the combined detector, respectively. The *a posteriori* probabilities of the information bits can also be computed to make the hard decisions at the output of the decoder after each iteration.

III. Design using EXIT Charts

In order to examine whether an iterative demodulation and decoding system can achieve near-capacity, one needs to take into account the convergence behavior in the turbo pinch-off, or water-fall, region, where a significant BER decrease is observed over iterations (please see [24] and references therein for detailed discussions). This section analyzes the convergence property of the proposed scheme at the turbo pinch-off region by means of extrinsic information transfer (EXIT) chart [10]. Following the same notations as in [10], let I_{A1} and I_{E1} denote the mutual information between the *a priori* LLR and the transmitted coded bit, and between extrinsic LLR and the transmitted coded bit at the input and output of the detector, respectively. Similarly, let I_{E2} and I_{A2} be the mutual information representing the *a priori* knowledge and the extrinsic information of the coded bits at the input and output of the SISO decoder. After being deinterleaved, the extrinsic output of the detector is used as the *a priori* input to the decoder, i.e., $I_{A2} = I_{E1}$. Furthermore, after being interleavered, the extrinsic information of the decoder becomes the *a priori* information to be provided to the detector, i.e., $I_{A1} = I_{E2}$.

In the following, with the representation of rate-1 linear block code together with 1-D mapping as a multi-D mapping ξ, a simple design criterion on the bit-wise mutual information with perfect *a priori* information $I_{E_1}(I_{A_1} = 1)$ is first derived. An optimal rate-1 linear block code is further developed for each 1-D mapping to maximize $I_{E_1}(I_{A_1} = 1)$. The difference between the conventional detector with Gray mapping employed in coded modulation systems using powerful turbo-like codes [3], [4], [8], [9] and the combined detector considered in this paper is then demonstrated with the aid of EXIT curves. Finally, a combination of the combined detector and a mixture of simple convolutional or repetition decoders, with which close-capacity performance can be achieved, is proposed by having the combined detector EXIT curve matched to the decoder EXIT curve. We only consider the same rate-1/2 component codes, which results in an overall rate $r_c = 1/2$ outer mixed code. The analysis and design can be straightforwardly extended to other code rates. The ratio of energy per information bit at the receiver over noise power, E_b/N_0, is defined as [3], [4]:

$$E_b/N_{0(\text{dB})} = E_s/N_{0(\text{dB})} + 10\log 10\frac{1}{r_c N_t m}, \tag{5}$$

where E_s is total energy used over N_t transmit antennas.

A. Bitwise Mutual Information with Perfect A Priori Information of the Combined Detector

For a given constellation $\mathbf{\Psi}$ and mapping rule ξ, the bitwise mutual information with perfect *a priori* information $I_{E_1}(I_{A_1} = 1)$ can be calculated as follows:

$$I_{E_1}(I_{A_1} = 1) = \frac{1}{Q2^Q}\sum_{\boldsymbol{s}\in\mathbf{\Psi}}\sum_{k=1}^{Q} I_k(\boldsymbol{s}, \boldsymbol{p}), \tag{6}$$

where $I_k(\boldsymbol{s}, \boldsymbol{p})$ is the average mutual information of a BPSK-like constellation consisting of two signal points $\boldsymbol{s}$ and $\boldsymbol{p}$ whose labels differ in only 1 bit at position k. Due to the symmetry of a BPSK-like constellation, the conditional $I_k(\boldsymbol{s}, \boldsymbol{p})|\boldsymbol{h}$ for a given channelization $\boldsymbol{h}$ can be expressed as:

$$I_k(\boldsymbol{s}, \boldsymbol{p})|\boldsymbol{h} = 1 - \left[\frac{1}{(\pi N_0)}\int_{r\in\mathcal{C}} \exp\left(-\frac{||r - \boldsymbol{h}^\top\cdot\boldsymbol{s}||^2}{N_0}\right) \times \log\left(1 + \exp\left(\frac{||r - \boldsymbol{h}^\top\cdot\boldsymbol{s}||^2 - ||r - \boldsymbol{h}^\top\cdot\boldsymbol{p}||^2}{N_0}\right)\right)\mathrm{d}r\right]. \tag{7}$$

By using the symmetric cut-off rate and Jensen inequality as similar to the analysis in [25], $I_k(\boldsymbol{s}, \boldsymbol{p})$ can be approximated as:

$$\begin{aligned} I_k(\boldsymbol{s}, \boldsymbol{p}) &\sim 1 - \log\left(1 + E_{\boldsymbol{h}}\left[\exp\left(-\frac{||\boldsymbol{h}^\top\cdot(\boldsymbol{s}-\boldsymbol{p})||^2}{4N_0}\right)\right]\right) \\ &= 1 - \log\left(1 + \frac{4N_0}{4N_0 + ||\boldsymbol{s}-\boldsymbol{p}||^2}\right). \end{aligned} \tag{8}$$

By substituting $I_k(\boldsymbol{s}, \boldsymbol{p})$ from (8) into (6), it can be seen that an optimal mapping rule ξ that maximizes $I_{E_1}(I_{A_1} = 1)$ is the mapping in which two signal points $\boldsymbol{s}$ and $\boldsymbol{p}$ whose labels differ in only 1 bit should be placed as far apart as possible in terms of the Euclidean distance. In the next subsection, in combining with either anti Gray or Gray mapping, an optimal rate-1 code is introduced to maximize $I_{E_1}(I_{A_1} = 1)$.

Digital Object Identifier: 10.4108/ICST.BROADNETS2009.7271
http://dx.doi.org/10.4108/ICST.BROADNETS2009.7271

B. Optimal Rate-1 Linear Block Codes

Without loss of generality, assume that the coordinates of the four QPSK symbols are $[+1,+1]$, $[+1,-1]$, $[-1,+1]$, and [-1,-1]. By representing the super constellation $\boldsymbol{\Psi}$ as a hypercube in N_t-D signal space, it was shown in [20] that for any symbol $\boldsymbol{s}$, there is only one symbol $\boldsymbol{p}$ at the largest squared Euclidean distance $4Q$ to $\boldsymbol{s}$. Furthermore, there are Q symbols $\{\boldsymbol{p}\}$ at the second largest squared Euclidean distance $4(Q-1)$ to $\boldsymbol{s}$. This implies the following upper bound on $I_{E_1}(I_{A_1}=1)$:

$$\begin{aligned} I_{E_1}(I_{A_1}=1) &\leq 1-\frac{1}{Q}\left[\log\left(1+\frac{N_0}{N_0+Q}\right)\right. \\ &+ \left.(Q-1)\log\left(1+\frac{N_0}{N_0+Q-1}\right)\right]. \quad (9) \end{aligned}$$

It is simple to see that a mapping rule ξ that satisfies the following condition achieves the equality in (9):

Condition 1: For any symbol $\boldsymbol{s}\in\boldsymbol{\Psi}$, let $\boldsymbol{\Psi_s}$ be a set of Q symbols $\{\boldsymbol{p}\}$ whose labels differ in only 1 bit to that of $\boldsymbol{s}$. In $\boldsymbol{\Psi_s}$, there are one symbol at squared Euclidean distance $4Q$ and $(Q-1)$ symbols at squared Euclidean distances $4(Q-1)$ to $\boldsymbol{s}$.

When combining with an 1-D mapping, a rate-1 code $\boldsymbol{G}$ is called *optimal* if it is linear and the combination leads to a multi-D mapping ξ that satisfies *Condition 1*. In the following, this optimal code is determined for both anti-Gray and Gray mappings. For convenience, the notations $\boldsymbol{W}$ and $\boldsymbol{F}$ are used to indicate rate-1 code for anti-Gray and Gray mappings, respectively.

1) Optimal codes for anti-Gray mapping: When anti-Gray mapping is used, it is straightforward to verify that a group of 2 binary bits (b_{2i-1},b_{2i}), $1\leq i\leq N_t$, shall be mapped to a QPSK symbol $s_i=[2(b_{2i-1}\oplus b_{2i})-1, 2b_{2i-1}-1,]$, where $\oplus$ denotes GF(2) addition. As a result, a symbol $\boldsymbol{s}\in\boldsymbol{\Psi}$ with label $\boldsymbol{v}$ carrying Q bits $\boldsymbol{b}$, $\boldsymbol{b}=\boldsymbol{G}\cdot\boldsymbol{v}$, can be represented as:

$$\boldsymbol{s}=[2(b_1\oplus b_2)-1, 2b_1-1, \ldots, 2(b_{Q-1}\oplus b_Q)-1, 2b_{Q-1}-1]^\top. \quad (10)$$

One then has the following theorem concerning the optimal $\boldsymbol{W}$.

Theorem 1: Let $\boldsymbol{w}_k=[w_{1,k},\ldots,w_{Q,k}]^\top$ be the kth column of $\boldsymbol{W}$. If $\boldsymbol{W}$ is optimal then

$$[w_{2i-1,k}, w_{2i,k}]=[1,0] \quad (11)$$

for at least (N_t-1) values of i, $1\leq i\leq N_t$.

Proof: Consider two symbols $\boldsymbol{s}=[s_1,\ldots,s_{N_t}]^\top$ and $\boldsymbol{p}=[p_1,\ldots,p_{N_t}]^\top$ whose labels $\boldsymbol{v}$ and $\boldsymbol{y}$ differ in only 1 bit at position k. Also, let $\boldsymbol{b}=\boldsymbol{W}\cdot\boldsymbol{v}$ and $\boldsymbol{a}=\boldsymbol{W}\cdot\boldsymbol{y}$. It then follows that:

$$\boldsymbol{b}\oplus\boldsymbol{a}=\boldsymbol{W}\cdot(\boldsymbol{v}\oplus\boldsymbol{y})=\boldsymbol{w}_k. \quad (12)$$

Since $\boldsymbol{W}$ is optimal, $||\boldsymbol{s}-\boldsymbol{p}||^2\geq 4(Q-1)$. Equivalently, $||s_i-p_i||^2=8$ for at least (N_t-1) values of i, $1\leq i\leq N_t$. Furthermore, from (10), one has:

$$\begin{aligned} ||s_i-p_i||^2 &= 4\left((b_{2i-1}-a_{2i-1})^2\right. \\ &+ \left.((b_{2i-1}\oplus b_{2i})-(a_{2i-1}\oplus a_{2i}))^2\right). \quad (13) \end{aligned}$$

It can be observed from (13) that $||s_i-p_i||^2=8$ if and only if $[b_{2i-1}\oplus a_{2i-1}, b_{2i}\oplus a_{2i}]=[1,0]$. Combining this result with (12) proves *Theorem 1*.

Based on *Theorem 1*, the next theorem provides an optimal $\boldsymbol{W}$ for anti-Gray mapping.

Theorem 2: For anti-Gray mapping, the entries of the optimal rate-1 block code $\boldsymbol{W}$ are given as:

$$[w_{2i-1,k}, w_{2i,k}]= \begin{cases} [1,0], & k=1, 1\leq i\leq N_t \\ [1,0], & 1<k\leq Q, i\neq (k+1) \text{ div } 2, 1\leq i\leq N_t \\ [0,1], & 1<k\leq Q, k \bmod 2=0, i=(k+1) \text{ div } 2 \\ [1,1], & 1<k\leq Q, k \bmod 2=1, i=(k+1) \text{ div } 2 \end{cases} \quad (14)$$

Proof: The linear property of $\boldsymbol{W}$ can be proved as follows. Let $\boldsymbol{m}=[m_1,\ldots,m_Q]^\top$ be a vector of Q binary bits and $m=m_1\oplus m_2\oplus\ldots\oplus m_Q$. Consider the following linear combination:

$$\boldsymbol{x}=m_1\boldsymbol{w}_1\oplus m_2\boldsymbol{w}_2\oplus\ldots\oplus m_Q\boldsymbol{w}_Q. \quad (15)$$

It then follows from (14) that:

$$\begin{aligned} \boldsymbol{x} &= [m\oplus m_2, m_2, \ldots, m\oplus m_{2i}, m_{2i-1}\oplus m_{2i}, \\ &\quad \ldots, m_Q, m_{Q-1}\oplus m_Q]^\top. \quad (16) \end{aligned}$$

Therefore, $\boldsymbol{x}=\boldsymbol{0}$ if and only if $\boldsymbol{m}=\boldsymbol{0}$. As a result, $\boldsymbol{W}$ is linear.

The optimality of $\boldsymbol{W}$ then follows readily from *Theorem 1*. In particular, let $\boldsymbol{s}$ and $\boldsymbol{p}$ be two symbols whose label differ in only 1 bit at position k. Consider two separate cases of k as follows:

- If $k=1$, it can be verified that $||s_i-p_i||^2=8$ for all $1\leq i\leq N_t$. This makes $||\boldsymbol{s}-\boldsymbol{p}||^2=4Q$
- If $k>1$, $||s_i-p_i||^2=8$ for all $1\leq i\leq N_t$ but $i=(k+1)$ div 2. When $i=(k+1)$ div 2, it follows from (14) and (13) that $||s_i-p_i||^2=4$. Therefore, $||\boldsymbol{s}-\boldsymbol{p}||^2=4(Q-1)$.

Theorem 2 is thus proved.

Besides the optimal $\boldsymbol{W}$ in (14), it is worth noting that by permuting any two columns of $\boldsymbol{W}$, another optimal code can be also obtained. The proof is straightforward and omitted here for brevity of the presentation.

2) Optimal codes for Gray mapping: For a given optimal $\boldsymbol{W}$ in (14), define $\boldsymbol{F}$ as a $Q\times Q$ matrix over GF(2) whose elements are:

$$\begin{cases} f_{2i-1,k}=w_{2i-1,k}\oplus w_{2i,k} \\ f_{2i,k}=w_{2i-1,k} \end{cases} \quad (17)$$

The following theorem states the optimality of $\boldsymbol{F}$.

Theorem 3: The use of rate-1 code $\boldsymbol{F}$ in (17) together with Gray mapping results in the same mapping rule ξ attainted by combining rate-1 code $\boldsymbol{W}$ in (14) and anti-Gray mapping. Consequently, $\boldsymbol{F}$ in (17) is optimal for Gray mapping.

Proof: Let $\boldsymbol{v}$ be a vector of binary inputs. When $\boldsymbol{W}$ in (14) is used together with anti-Gray mapping, a symbol $\boldsymbol{s}\in\boldsymbol{\Psi}$ with label $\boldsymbol{v}$ carrying Q bits $\boldsymbol{b}$, $\boldsymbol{b}=\boldsymbol{G}\cdot\boldsymbol{v}$, is given in (10). On the other hand, with rate-1 code $\boldsymbol{F}$ followed by Gray mapping, a

Digital Object Identifier: 10.4108/ICST.BROADNETS2009.7271
http://dx.doi.org/10.4108/ICST.BROADNETS2009.7271

symbol $\boldsymbol{p} \in \boldsymbol{\Psi}$ carrying Q bits $\boldsymbol{a}$, $\boldsymbol{a} = \boldsymbol{F} \cdot \boldsymbol{v}$, can be expressed as:

$$\boldsymbol{p} = [2a_1 - 1, 2a_2 - 1, \ldots, 2a_{Q-1} - 1, 2a_Q - 1]^\top. \quad (18)$$

From (17), one has:

$$\begin{cases} a_{2i-1} = \boldsymbol{f}^{(2i-1)} \cdot \boldsymbol{v} = \left(\boldsymbol{w}^{(2i-1)} \oplus \boldsymbol{w}^{(2i)}\right) \cdot \boldsymbol{v} = b_{2i-1} \oplus b_{2i} \\ a_{2i} = \boldsymbol{f}^{(2i-1)} \cdot \boldsymbol{v} = \boldsymbol{w}^{(2i-1)} \cdot \boldsymbol{v} = b_{2i-1} \end{cases} \quad (19)$$

where $\boldsymbol{f}^{(k)}$ and $\boldsymbol{w}^{(k)}$ are the kth rows of $\boldsymbol{F}$ and $\boldsymbol{W}$, respectively. It then follows from (10), (18), and (19) that $\boldsymbol{s} = \boldsymbol{p}$. It means that a combination of either $\boldsymbol{F}$ and Gray mapping or $\boldsymbol{W}$ and anti-Gray mapping leads to the same mapping rule ξ. *Theorem 3* is proved.

Combining the above results, it can be concluded that the combination of rate-1 code $\boldsymbol{W}$ in (14) followed by anti-Gray mapping is equivalent to the combination of rate-1 code $\boldsymbol{F}$ in (17) and Gray mapping. Furthermore, these combinations maximize $I_{E_1}(I_{A_1} = 1)$.

C. EXIT Curves of the Conventional and Combined Detectors

Figure 2 shows EXIT curves of the conventional detector using Gray mapping and combined detector at $E_b/N_0 = 5$dB with $N_t = 4$ and $N_t = 6$ transmit antennas. For a conventional detector with Gray mapping, the EXIT curve exhibits a steep slope. This phenomenon causes a performance degradation when Gray mapping is used together with turbo codes [4], [7]. In the case of the combined detector, it can be seen that the bitwise mutual information with perfect *a priori* information $I_{E_1}(I_{A_1} = 1)$ can be significantly improved over that of the conventional detector. However, since the proposed block codes are of rate 1, the areas under the EXIT curves of the combined detector and conventional detector must be equal [26]. Consequently, it can be observed from Fig. 2 that the combined detector's EXIT curve exhibits even much higher slope over that of the conventional detector, with a very large mutual information at the right end of the curve. As shown in the next subsection, this makes the combination of either rate-1 code $\boldsymbol{W}$ in (14) with anti-Gray mapping or rate-1 code $\boldsymbol{F}$ in (17) with Gray mapping a perfect match to a simple outer mixed codes, which also have decayed EXIT curves. More interestingly, near-capacity performance can be achieved.

D. EXIT Curve Matching

This subsection applies EXIT chart technique [10] to select a suitable mixed code for the combined detector. By using EXIT charts, both EXIT curves of the combined detector and decoder are placed in the same graph, but the axes of the EXIT curve of the decoder are swapped [10] so that the convergence behavior of the concatenation scheme can be well visualized. It should be mentioned that for the system under consideration, the EXIT curve of a rate-r_c mixed code does not depend on SNR and always crosses the middle point $(0.5, r_c)$ [10].

We first examine the case with $N_t = 4$ as similar to [4]. Figure 3 plots the EXIT curve of the combined detector at E_b/N_0=7.55dB and the EXIT curves of two simple rate-1/2 codes, a 2-state convolutional code with generator polynomials

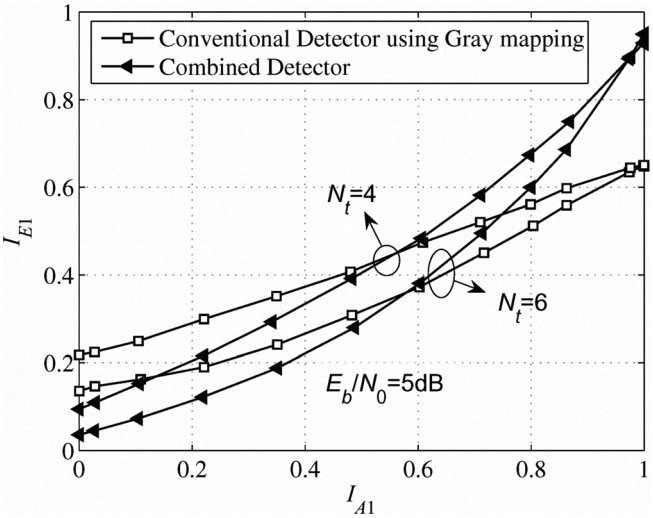

Fig. 2. The MIMO detector and combined detector EXIT curves at E_b/N_0=5dB.

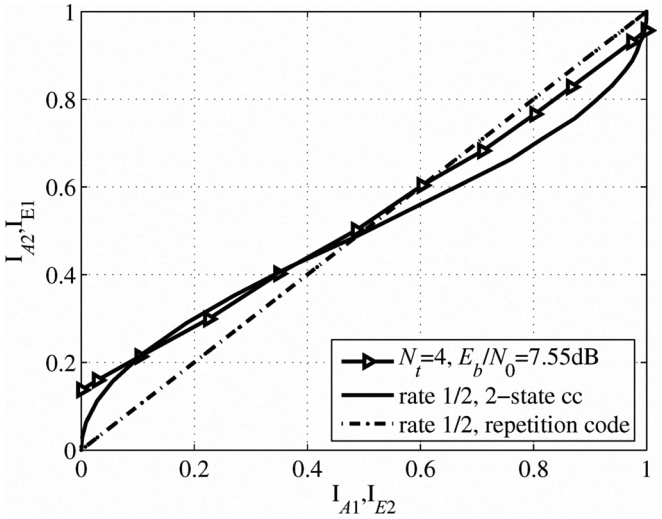

Fig. 3. EXIT curves of the combined detector with $N_t = 4$ transmit antennas at E_b/N_0=7.55dB, the rate-1/2, 2-state convolutional code (cc), and the rate-1/2 repetition code.

$\mathbf{g}_1 = [1, 1]$ and $\mathbf{g}_2 = [1, 0]$, and a repetition code. Note that the rate-1/2 repetition code is the simplest possible code, whereas the rate-1/2 2-state convolutional code is the simplest convolutional code. The above SNR is chosen to make sure that the middle point of the detector EXIT curve $I_{E_1}(0.5)$ is larger than 0.5. It is clear from Fig. 3 that the EXIT curve of the standard rate-1/2, 2-state convolutional code does not fit well to the detector EXIT curve, since the two EXIT curves quickly intersect and the intersection point falls in the lower left quadrant of the EXIT plane. Because the EXIT curve of a more powerful rate-1/2 convolutional code exhibits a sharper slope at the beginning, it is straightforward to see that there does not exist any suitable rate-1/2 convolutional code for the system. The EXIT curve of rate-1/2 repetition code intersects the combined detector EXIT curve in the upper right quadrant

Digital Object Identifier: 10.4108/ICST.BROADNETS2009.7271
http://dx.doi.org/10.4108/ICST.BROADNETS2009.7271

of the EXIT plane, but at a low mutual information, which does not guarantee low BER.

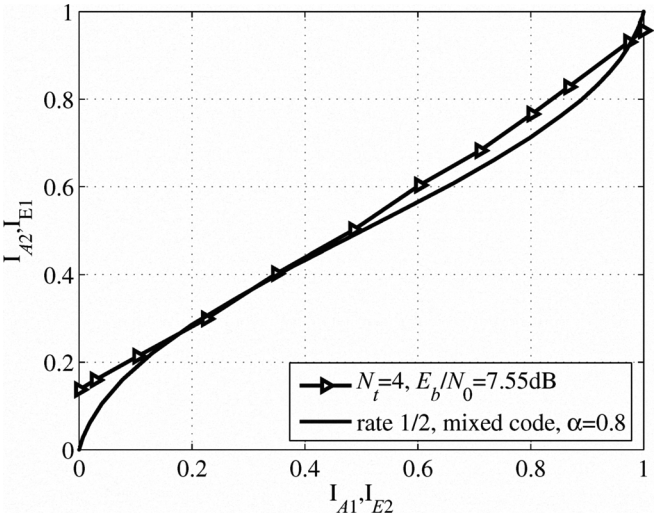

Fig. 4. EXIT charts of the combined detector with $N_t = 4$ at E_b/N_0=7.55dB and a rate-1/2 mixed code of 2-state cc and repetition code with code doping ratio $\alpha = 0.8$.

To overcome the above disadvantages, a mixed code of the two above codes can be used to achieve better curve matching. In particular, Fig. 4 shows the EXIT curve of the combined detector at $E_b/N_0 = 7.55$dB and the EXIT curve of a mixture of 2-state convolutional code (cc) and repetition code with code doping ratio $\alpha = 0.8$. It is interesting to see that the EXIT curve of this mixed code matches very well to the detector EXIT curve. The two EXIT curves do not intersect until reaching the ending point $I_{A_1}(1)$ with very high mutual information, leading to a low BER. This match is very similar to that obtained in [4], [9] using an irregular LDPC or RA code and Gray mapping alone. Furthermore, this curve fit happens close to the capacity limit, which is at $E_b/N_0 = 6.65$dB.

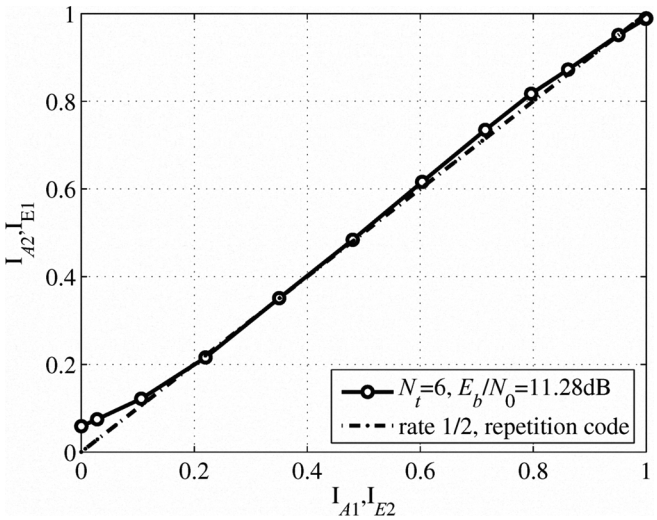

Fig. 5. EXIT charts of the combined detector with $N_t = 6$ at E_b/N_0=11.28dB and a rate-1/2 repetition code.

In the case of using a larger number of transmit antenna, it can be seen from Fig. 2 that the combined detector EXIT curves experience much higher slope. This suggests that even a simpler code could be used for a good convergence. In particular, Fig. 5 shows the EXIT curve of the combined detector when N_t=6 at E_b/N_0=11.28dB. Note that the corresponding capacity limit is at E_b/N_0=10.77dB. Also plotted in Fig. 5 is the EXIT curve of a rate-1/2 repetition code. It is observed from Fig. 5 that the combined detector EXIT curve of the N_t=6 setup fits well to that of the rate-1/2 repetition code, which is the simplest possible code. More impressively, this curve match is achieved at only 0.5dB away from the capacity limit.

Similar results are also obtained when the number of transmit antenna increases. Those results are, however, omitted here for brevity of the presentation.

IV. Illustrative Results

This section provides simulation results to verify the analysis made in the previous sections and to demonstrate the excellent performance achieved by the proposed systems. A random interleaver of length 3×10^5 is used for all systems under consideration. Each point in the BER curves is simulated with 6×10^6 to 10^9 coded bits.

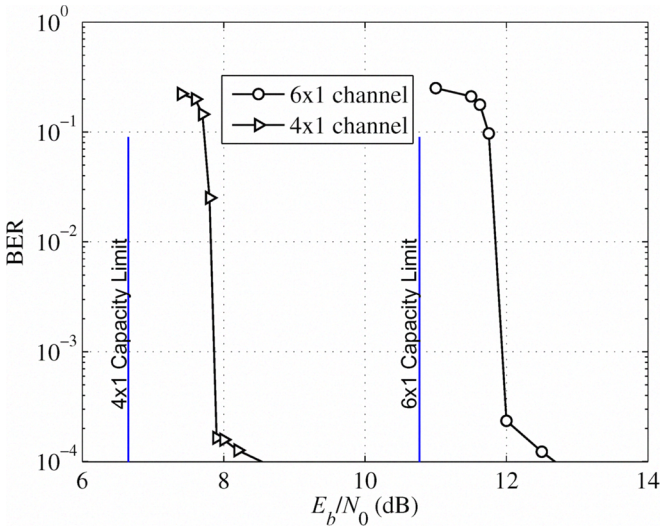

Fig. 6. BER performances with 50 iterations of the proposed systems equipped with $N_t = 6$ and $N_t = 4$ transmit antennas, and $N_r = 1$ receive antenna. The outer codes are rate-1/2, repetition code and rate-1/2 mixed code of rate-1/2 standard 2-state convolutional code and rate-1/2 repetition code with $\alpha = 0.8$, respectively.

Figure 6 plots the BER performance with 50 iterations of the 6×1 and 4×1 systems. The corresponding outer codes for the two systems are the rate-1/2, repetition code and the rate-1/2 mixed code comprised of the rate-1/2 standard 2-state convolutional code and the rate-1/2 repetition code with $\alpha = 0.8$. The spectral efficiency for each system is therefore 6 bits/channel use and 4 bits/channel use, respectively. It can be seen from Fig. 6 that the analytical results obtained by EXIT charts agree with the BER curves. In particular, the turbo pinch-off region happens around E_b/N_0=7.8dB and

Digital Object Identifier: 10.4108/ICST.BROADNETS2009.7271
http://dx.doi.org/10.4108/ICST.BROADNETS2009.7271

E_b/N_0=11.6dB over 4×1 and 6×1 channels, respectively, which is only about 1dB from the capacity limit in both channels. Apparently, the results appear impressive for such simple systems.

V. Conclusions

This paper proposed a novel coded modulation scheme over multiple-input single-output channels with QPSK. The scheme is based on a concatenation of a simple outer mixed code and a short rate-1 linear block code followed by either 1-D anti-Gray or Gray mapping. The optimal rate-1 code was first developed to maximize the bit-wise mutual information with perfect *a priori* information. It has then been shown through EXIT chart analysis that the proposed system achieves near-capacity in the turbo pinch-off region using simple outer binary codes. The proposed system is therefore an attractive alternative for other coded modulation schemes over wireless fading channels, especially in the downlink of a cellular system.

References

[1] G. J. Foschini, "Layered spacetime architecture for wireless communication in a fading environment when using multi-element antennas," *Bell Labs. Tech. J.*, vol. 1, pp. 41–59, Feb. 1996.

[2] I. E. Telatar, "Capacity of multi-antenna Gaussian channels," *European Trans. Telecommun. Related Technol.*, vol. 10, pp. 585–595, Nov. 1999.

[3] B. M. Hochwald and S. ten Brink, "Achieving near-capacity on mutiple-antenna channel," *IEEE Trans. Commun.*, vol. 51, pp. 389–399, Mar. 2003.

[4] S. ten Brink, G. Kramer, and A. Ashikhmin, "Design of Low-Density Parity-Check Codes for Modulation and Detection," *IEEE Trans. Commun.*, vol. 52, pp. 670–678, Apr. 2004.

[5] E. Zehavi, "8-PSK trellis codes for a Rayleigh fading channel," *IEEE Trans. Commun.*, vol. 40, pp. 873–883, May 1992.

[6] G. Caire, G. Taricco, and E. Biglieri, "Bit-interleaved coded modulation," *IEEE Trans. Inform. Theory*, vol. 44, pp. 927–946, May 1998.

[7] S. ten Brink and B. M. Hochwald, "Detection Thresholds of Iterative MIMO Processing," in *Proc. IEEE Int. Symp. Inform. Theory*, (Lausanne, Switzerland), p. 22, July 2002.

[8] J. Hou, P. H. Siegel, and L. B. Milstein, "Design of multi-input multi-output systems based on low-density parity-check codes," *IEEE Trans. Commun.*, vol. 53, pp. 601–611, Apr. 2005.

[9] S. ten Brink and G. Kramer, "Design of Repeat Accumulate Codes for Iterative Detection and Decoding," *IEEE Trans. Signal Process.*, vol. 51, pp. 2764–2772, Nov. 2003.

[10] S. ten Brink, "Designing iterative decoding schemes with the extrinsic information chart," *AEU Int. J. Electron. Commun*, vol. 54, pp. 389–398, Sept. 2000.

[11] S. ten Brink, "Design of repeat-accumulate codes for iterative detection and decoding," *Electronics Letters*, vol. 36, pp. 1293–1294, July 2000.

[12] V. Tarokh, N. Seshadri, and A. R. Calderbank, "Space-time codes for high data rate wireless communication: Performance criterion and code construction," *IEEE Trans. Inform. Theory*, vol. 44, pp. 744–765, Mar. 1998.

[13] V. Tarokh, H. Jafarkhani, and A. R. Calderbank, "Space-time block codes from orthogonal designs," *IEEE Trans. Inform. Theory*, vol. 45, pp. 1456–1467, July 1999.

[14] B. Hassibi and B. Hochwald, "High-rate codes that are linear in space and time," *IEEE Trans. Inform. Theory*, vol. 48, pp. 1804–1824, July 2002.

[15] H. E. Gamal and M. O. Damen, "Universal spacetime coding," *IEEE Trans. Inform. Theory*, vol. 49, pp. 1097–1119, May 2003.

[16] N. H. Tran, T. Le-Ngoc, T. Matsumoto, and H. H. Nguyen, "Achieving near-capacity performance on multiple-antenna channels with a simple concatenation scheme," submitted to *IEEE Trans. on Communications*, 2009.

[17] N. H. Tran, T. Le-Ngoc, T. Matsumoto, and H. H. Nguyen, "Achieving close-capacity performance with simple concatenation scheme on multiple-antenna channels," in *Proc. IEEE Global Telecommun. Conf.*, (Honolulu, Hawaii, USA), pp. 1–6, Dec. 2009.

[18] S. ten Brink, "Code Doping for Triggering Iterative Decoding Convergence," in *Proc. IEEE Int. Symp. Inform. Theory*, (Washington, DC, USA), p. 235, June 2001.

[19] M. Tuchler and J. Hagenauer, "EXIT charts of irregular codes," in *Proc. Conference on Information Sciences and Systems*, (Princeton University, USA), pp. 1–6, Mar. 2002.

[20] N. H. Tran and H. H. Nguyen, "Design and performance of BICM-ID systems with hypercube constellations," *IEEE Trans. on Wireless Commun.*, vol. 5, pp. 1169–1179, May 2006.

[21] N. Gresset, J. Boutros, and L. Brunel, "Multidimensional mappings for iteratively decoded BICM on multiple-antenna channels," *IEEE Trans. Inform. Theory*, vol. 51, pp. 3337–3346, Sept. 2005.

[22] L. R. Bahl, J. Cocke, F. Jelinek, and J. Raviv, "Optimal decoding of linear codes for minimizing symbol error rate," *IEEE Trans. Inform. Theory*, vol. IT-20, pp. 284–287, Mar. 1974.

[23] S. Benedetto, D. Divsalar, G. Montorsi, and F. Pollara, "A soft-input soft-output APP module for iterative decoding of concatenated codes," *IEEE Commun. Letters*, vol. 1, pp. 22–24, Jan 1997.

[24] S. ten Brink, "Convergence Behavior of Iteratively Decoded Parallel Concatenated Codes," *IEEE Trans. Commun.*, vol. 49, pp. 1727–1737, Oct. 2001.

[25] E. Baccarelli and A. Fasano, "Some Simple Bounds on the Symmetric Capacity and Outage Probability for QAM Wireless Channels with Rice and Nakagami Fadings," *IEEE J. Select. Areas in Commun.*, vol. 18, pp. 361–368, Mar. 2000.

[26] J. Hagenauer, "The EXIT Chart - Introduction to extrinsic information transfer in iterative processing," in *12th European Signal Processing Conference (EUSIPCO)*, pp. 1541–1548, 2004.

Digital Object Identifier: 10.4108/ICST.BROADNETS2009.7271
http://dx.doi.org/10.4108/ICST.BROADNETS2009.7271